



HAL
open science

Characterization of the Denaturation of Bovine Serum Albumin (BSA) Protein by Means of a Differential-Mode Microwave Microfluidic Sensor Based on Slot Resonators

Jonathan Munoz-Enano, Olivia Peytral-Rieu, Paris Velez, David Dubuc,
Katia Grenier, Ferran Martin

► To cite this version:

Jonathan Munoz-Enano, Olivia Peytral-Rieu, Paris Velez, David Dubuc, Katia Grenier, et al.. Characterization of the Denaturation of Bovine Serum Albumin (BSA) Protein by Means of a Differential-Mode Microwave Microfluidic Sensor Based on Slot Resonators. *IEEE Sensors Journal*, 2022, 22 (14), pp.14075 - 14083. 10.1109/JSEN.2022.3181542 . hal-03714052

HAL Id: hal-03714052

<https://laas.hal.science/hal-03714052v1>

Submitted on 5 Jul 2022

HAL is a multi-disciplinary open access archive for the deposit and dissemination of scientific research documents, whether they are published or not. The documents may come from teaching and research institutions in France or abroad, or from public or private research centers.

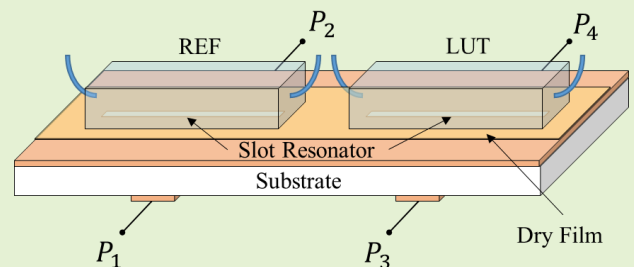
L'archive ouverte pluridisciplinaire **HAL**, est destinée au dépôt et à la diffusion de documents scientifiques de niveau recherche, publiés ou non, émanant des établissements d'enseignement et de recherche français ou étrangers, des laboratoires publics ou privés.

Characterization of the Denaturation of Bovine Serum Albumin (BSA) Protein by Means of a Differential-Mode Microwave Microfluidic Sensor Based on Slot Resonators

Jonathan Muñoz-Enano, *Student Member, IEEE*, Olivia Peytral-Rieu, *Student Member, IEEE*, Paris Vélez, *Senior Member, IEEE*, David Dubuc, *Member, IEEE*, Katia Grenier, *Member, IEEE*, and Ferran Martín, *Fellow, IEEE*

Abstract—This paper presents a differential-mode microwave microfluidic sensor useful for the characterization/detection of the denaturation of Bovine Serum Albumin (BSA), a protein with numerous biochemical applications, caused by a chaotropic agent, specifically, urea. The sensor consists of a pair of uncoupled microstrip lines, each one loaded with a transversally oriented slot resonator, etched in the ground plane. The sensor is a device able to detect permittivity changes in the so-called material under test (MUT), or liquid under test (LUT), as compared to a reference (REF) material/liquid. However, since the changes in the permittivity of the BSA caused by the denaturation process are partially obscured by the presence of the urea in the LUT, a protocol to separate the effects of the urea in the sample is proposed. According to such protocol, two different BSA samples, with different concentrations, are needed. It is shown that, with such a method, the denaturation process can be detected and characterized through the so-called hydration contrast, related to the measured difference of the output variables (the cross-mode transmission coefficient) in both BSA samples. The reported protocol and denaturation detection method based on differential-mode microwave sensing, which has never been reported so far, provides hydration contrasts of 0.06 for 6M urea concentrations.

Index Terms—Bovine serum albumin (BSA), defect-ground-structure (DGS), differential sensor, microfluidics, microwave sensor, protein denaturation, slot resonator.



I. INTRODUCTION

MICROWAVE sensors have been applied to the characterization of a wide diversity of materials and substances, as well as to the measurement of variables of different type, including physical, chemical, and biological variables. Among them, planar microwave sensors have been the subject of an intensive research activity in recent years, caused by the advantages of such sensors over non-planar sensors (e.g., waveguide or cavity sensors), including lower cost and profile, compatibility with additive and subtractive fabrication processes, potential for the implementation of conformal sensors and “green” sensors, and compatibility with other technologies, in particular microfluidics, among others.

This work was supported by MCIN/AEI 10.13039/501100011033, Spain, through the projects PID2019-103904RB-I00 (ERDF European Union) and PDC2021-121085-I00 (European Union Next Generation EU/PRTR), by the AGAUR Research Agency, Catalonia Government, through the project 2017SGR-1159, and by Institució Catalana de Recerca i Estudis Avançats (who awarded Ferran Martín). J. Muñoz-Enano acknowledges Secretaria d'Universitats i Recerca (Gen. Cat.) and European Social Fund for the FI grant. This work was also partly supported as part of the MultiFAB project funded by FEDER European

Microwave sensors are devices sensitive to the dielectric properties of their surrounding medium, particularly, the permittivity. Nevertheless, there are many physical, chemical and biological variables that are intimately related to the permittivity. Therefore, microwave sensors are useful for a wide variety of applications, including moisture measurements [1]-[4], temperature measurements [3]-[5],[6] determination of motion variables [7]-[17], defect detection [18]-[19], solute concentration measurements in liquid solutions [20]-[24], liquid characterization [25], electrolyte concentration measurements in bio-samples [26],[27], non-destructive and label-free cellular analysis [28]-[30], or dielectric spectroscopy of biomolecules [31]-[37], to cite some of them. In many of the previous applications where the samples are liquids, the planar

Regional Funds and French Région Occitanie (grant agreement number 16007407/MP0011594) and by LAAS-CNRS micro and nanotechnologies platform, a member of the French RENATECH network.

J. Muñoz-Enano, P. Vélez, and F. Martín are with GEMMA/CIMITEC, Departament d'Enginyeria Electrònica, Universitat Autònoma de Barcelona, 08193 Bellaterra, Spain. (e-mail: Ferran.Martin@uab.es).

O. Peytral-Rieu D. Dubuc and K. Grenier are with MH2F, LAAS-CNRS, 31031 Toulouse, France (e-mail: grenier@laas.fr).

sensors are combined with microfluidic channels [18],[20]-[24],[26],[27] in order to drive the liquid under test (LUT) to the sensitive region (nevertheless, there are examples of sensors based on small liquid containers [25], as well as sensors where the sensitive element is a probe that can be submersed in the LUT [38]-[40]). In this paper, we report a microwave microfluidic sensor devoted to the detection and characterization of the hydration modification in a protein, particularly Bovine Serum Albumin (BSA), subjected to a chaotropic agent, i.e., urea. The urea acts as a denaturing agent, disrupting the hydrogen bonding network between water molecules and reducing the stability of the native state of the protein by weakening the hydrophobic effect, thereby denaturing the protein and modifying the structure of the BSA from a fully folded macromolecule to an unstructured unfolded coil, as depicted in Fig. 1.

Usually, traditional techniques used to evaluate the denaturation of proteins are based on optical methods such as circular dichroism, UV-visible absorbance and fluorescence microscopy. Even if efficient, these techniques are delicate to use, suffer from rapidity and may also request labelling, thereby being costly and time-consuming. Demonstrating the possible detection of the denaturation of proteins with microwave sensing is consequently of great interest. It is expected that the dielectric properties of BSA change as consequence of denaturation. Thus, the use of microwave sensors seems to be an interesting approach for the detection of the denaturation process since microwave sensing is highly sensitive to water content and especially the ratio of bounded and free water molecules. However, the presence of the denaturing agent (urea) is expected to also generate a significant change in dielectric properties of the composite, actually a solution of BSA and urea. Thus, a method to cancel the effects of urea will be reported. The interest for the present study is justified by the fact that BSA constitutes a well-known molecule for chemists, and it is often chosen as a model since it can be subjected to simple and easy-to-control denaturation processes with different techniques, i.e., temperature, or a chaotropic agent, such as urea, the case considered in the present work. Additionally, it is present in blood plasma and circulatory system. It binds with ligand and contribute to 80% of the osmotic blood pressure, and is also responsible for maintaining blood pH [41]. Small changes in the local environment of a protein can cause structural changes and, thereby, affect the original function of the protein, which is of great interest in understanding folding/unfolding dynamics [42].

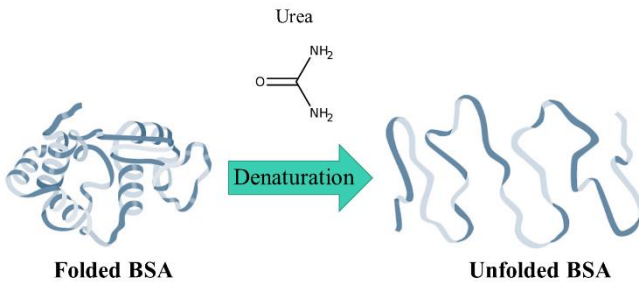


Fig. 1. Sketch showing the denaturation of BSA.

Concerning the proposed sensing structure, it is based on a differential-mode topology, where two uncoupled microstrip lines are loaded with transversally oriented slot resonators, the sensing elements. A differential-mode sensing scheme has been chosen because it has been found that significant sensitivities and very good resolutions result by considering the cross-mode transmission coefficient as the differential output variable (examples of these sensors are reported in [26],[27],[43]). Other differential sensors can be found in [44]-[46]. On the other hand, it has been demonstrated that DB-DGS-loaded and slot-loaded microstrip lines exhibit a very strong dependence of its resonance frequency with the dielectric constant of the material (solid or liquid) in contact with the resonator [47], and this is a key aspect in order to achieve high sensitivity in the cross-mode reflection coefficient when the sensor operates differentially. Additionally, differential sensors are robust to cross-sensitivities potentially caused by changing ambient factors (e.g., temperature or humidity), since these environmental variables are seen as common-mode stimuli by such sensors. By contrast single-ended sensors, typically based on frequency variation [25],[48]-[57] or phase variation [16],[19],[58]-[62], are less tolerant to the effects of changing ambient factors (though they are, in general, smaller).

The work is organized as follows. The topology, the circuit model and the working principle of the sensor are reported in Section II. Section III includes the fluidic part of the sensor and reports the first tests by considering the single-ended version of the slot-based sensor and different LUTs involved in this work, particularly DI water, phosphate-buffered saline (PBS), and two solutions of BSA in PBS. The characterization of the BSA denaturation caused by urea is the subject of Section IV. Finally, the main conclusions of the work are highlighted in Section V.

II. SENSOR TOPOLOGY, CIRCUIT MODEL AND WORKING PRINCIPLE

The topology of the single-ended version of the proposed slot-based sensor (excluding the fluidic channels) and the equivalent circuit model are depicted in Fig. 2. This sensor exhibits a notch in the frequency response dictated by the following frequency [63]

$$f_0 = \frac{1}{2\pi} \left(LC \frac{\epsilon_r + \epsilon_{MUT}}{\epsilon_r + 1} \right)^{-1/2} \quad (1)$$

where C and L are the capacitance and inductance, respectively, of the slot resonator in contact with air, ϵ_r is the dielectric constant of the substrate and ϵ_{MUT} is the dielectric constant of the material under test (MUT), or, in our specific case, liquid under test (LUT). In the model, G accounts for the dielectric losses of the substrate, whereas G_{MUT} and C_{MUT} model the presence of the MUT, contributing to the enhancement of the conductance, and capacitance of the slot resonator. The access lines to the slot resonator are described by the characteristic impedance Z_0 and electrical length βl , where β and l are the phase constant and length, respectively, of such lines. Note that the validity of the model is restricted to frequencies in the vicinity of slot resonance (around 1 GHz in the present work),

since the considered resonators (slots) are distributed elements. The choice of this frequency obeys a trade-off. At lower frequencies, larger sensor dimensions result. At higher frequencies, the measurements are more complex. In addition, the changes in the permittivity of the samples at this frequency are enough to be detected.

Note that the validity of (1) is subjected to the presence of thick enough substrate and LUT, to consider that the field lines generated by the slot resonator do not reach the opposite extreme of the substrate or LUT (semi-infinite substrate and MUT approximation). The relative sensitivity, a key figure of merit, is given by

$$S = \frac{1}{f_0} \frac{df_0}{d\varepsilon_{MUT}} \quad (2)$$

and, after some simple calculation, it can be expressed as

$$S = -\frac{1}{2} \frac{1}{(\varepsilon_r + \varepsilon_{MUT})} \quad (3)$$

From (3), we can deduce that, as reported in [63], the relative sensitivity does not depend on the geometry of the slot resonator. Moreover, for high dielectric constant MUTs, such as liquids (the MUT used in this work), the relative sensitivity is dominated by the dielectric constant of such MUT. Thus, the dielectric constant of the substrate has a small effect on the relative sensitivity of the sensor.

As mentioned, expressions (1) and (3) are valid provided the semi-infinite substrate and MUT approximations are satisfied. In practice, the MUT, or the LUT in our case, can be made thick enough, so that such approximation holds. However, it is not obvious that the substrate can be considered to be semi-infinite in the vertical direction, at least for the typical thicknesses of most considered commercial microwave substrates. Nevertheless, for finite substrates, expressions (1) and (3) are valid by replacing ε_r with $\varepsilon_{r,eq}$, the so-called equivalent dielectric constant of the substrate. Such equivalent dielectric constant was defined in [63] as the dielectric constant of an hypothetical semi-infinite substrate providing the same contribution to the capacitance of the slot resonator. Obviously

$\varepsilon_{r,eq} < \varepsilon_r$, but $\varepsilon_{r,eq} \rightarrow \varepsilon_r$ in the limit where the substrate thickness is thick enough, so that the semi-infinite approximation is valid. The equivalent dielectric constant depends on the ratio between the slot width and the substrate thickness, except for the semi-infinite substrate approximation, where $\varepsilon_{r,eq} = \varepsilon_r$, as indicated [63]. This means that if such approximation is not valid, the relative sensitivity given by (3) actually depends on the geometry of the sensing element. However, as it has been demonstrated in [63], the dependence is soft.

In differential-mode configuration, two independent sensing structures are used, one for the reference (REF) material, and the other one for the LUT. The topology of such four-port structure, based on a pair of identical microstrip lines, each one loaded with a slot resonator, is depicted in Fig. 3. The working principle in this case is mode conversion caused by symmetry disruption, very sensitive to the presence of unbalanced loads in the pair of sensing (slot resonator) elements. Namely, if the loads of both slot resonators are the same, the responses of both lines should be identical, in particular the transmission coefficients should satisfy $S_{21} = S_{43}$, and mode conversion does not arise (this aspect has been corroborated experimentally, with the bare, and hence balanced, structure, though the results are not shown). Nonetheless, if the REF and LUT resonators are loaded with different materials, or samples, $S_{21} \neq S_{43}$, and axial symmetry is truncated. The differential output variable in such sensors is typically the cross-mode transmission coefficient. Considering that the lines are uncoupled, the cross-mode transmission coefficient is given by [64],[65]

$$S_{21}^{DC} = \frac{1}{2} (S_{21} - S_{43}) \quad (4)$$

Inspection of (4) shows that, when both slot-loaded lines are identically loaded, or unloaded (i.e., they exhibit the same frequency response), mode conversion is prevented and the cross-mode transmission coefficient is (ideally) null. However, if the sensing slot resonators are loaded with different samples, mode conversion arises, and the magnitude of the cross-mode transmission coefficient is determined by the level of asymmetry. If the response of each individual line is quite sensitive to the presence of a material on top of the slot resonator, it is expected that a small perturbation in the LUT, with regard to the REF liquid, will result in a significant variation between the transmission coefficients of both lines, which will be reflected in the cross-mode transmission coefficient. Indeed, the slot resonators have been chosen as sensing elements since these resonant elements exhibit high relative sensitivity in their use as single-ended sensors, as demonstrated in [47],[63], thereby giving rise to a significant sensitivity of the cross-mode transmission coefficient with the differential dielectric constant, when the differential-mode counterpart is considered. Such high sensitivity of the cross-mode transmission coefficient with the differential dielectric constant, plus the benefits inherent to differential sensing, are the main reasons for choosing a differential-mode sensing scheme in this work.

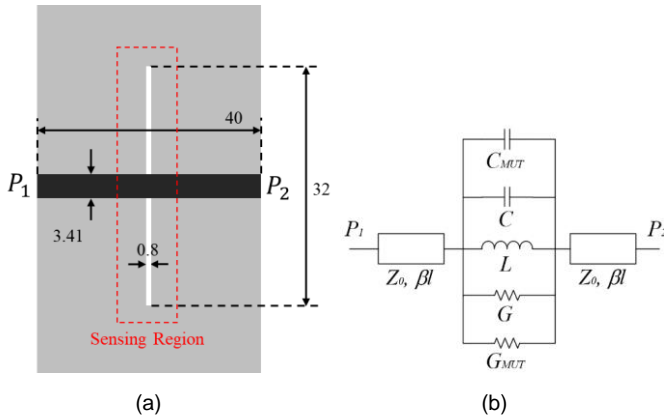


Fig. 2. Typical topology (a) and circuit model (b) of the proposed slot-based sensor. Dimensions are given in mm. The ground plane is depicted in grey colour.

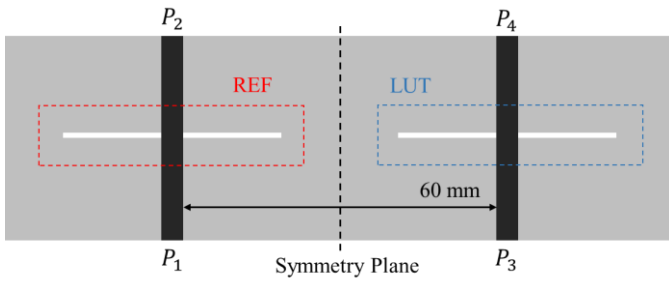


Fig. 3. Topology of the differential-mode four-port structure sensor based on a pair of microstrip lines loaded with slot resonators.

III. FLUIDIC PART AND VALIDATION TESTS

For the application of the sensor to the characterization of liquid samples, as those considered in the present work, it has been necessary to design fluidic channels with the corresponding accessories (in order to fix the channel to the sensor substrate and to inject the liquids in a controllable way). The fluidic channels have been fabricated by means of the *DWS J29+* 3D Printer using *DWS DS3000* biocompatible resin material, at 5.8 mm/h print speed and 50 μm layer height. The microfluidic tubing has been glued directly to the fluidic channel with cyanoacrylate glue. Figure 4 shows the picture of the fluidic channel (including dimensions). To attach the fluidic channel to the sensor, a 100 μm laser cut double-sided tape (*TESA 61532*) with the same dimensions as the fluidic channel has been used. Finally, to avoid substrate absorption, a 50 μm dry film of polymer (with the acronym DF and similar properties to the *SU-8* polymer, which is traditionally employed in microfluidics) with an estimated dielectric constant of 3.5 has been applied on top of the sensing region. The considered substrate for the sensor is the *Rogers RO4003C* with dielectric constant $\epsilon_r = 3.55$, thickness $h = 1.524$ mm and loss tangent $\tan\delta = 0.0022$.



Fig. 4. Photograph of the designed fluidic channel including fluidic accessories. The dimensions of the fluidic channels are (in mm): $l_{ch} = 35$, $W_{ch} = 6$ and $h_{ch} = 2$.

The first experimental validation tests have been carried out by considering only one half of the sensing structure, i.e., it has been demonstrated the functionality of the structure as a single-ended sensor. For that purpose, the fluidic channel has been loaded with different LUTs: (i) deionized (DI) water, (ii) phosphate-buffered saline (PBS) and (iii) solutions of BSA in PBS (at 1 and 2 mg/ml). For the PBS, 2.72 g of $(\text{KH}_2\text{PO}_4 + 12 \text{H}_2\text{O})$ and 7.16 g of Na_2HPO_4 were added in 200 mL of DI water to obtain the buffer solution at 200 mM and with a pH of 7.4. This solution was then diluted in DI water with a buffer/water ratio of 1:3 to obtain our phosphate buffer at 50 mM (millimolar) and a pH of 7.4. The pH measurement was

performed using a probe connected to a *Hanna Instruments HI2211* pH meter. The solution of BSA 2 mg/mL is prepared by dissolving 0.2 g of freeze-dried BSA in 100 mL of PBS and the solution of BSA 1 mg/mL by diluting the previous solution. These first experimental validation tests have had a twofold purpose: (i) to check if the sensor sensitivity is good enough, and (ii) to verify that there is not liquid leakage by using the 3D printed fluidic channels.

The measured transmission coefficient (magnitude) for the different LUTs is depicted in Fig. 5. The measurements have been carried out by means of the *Copper Mountain Technologies C1420* vector network analyzer with the sensor located on an anti-vibration table. For each sample, several measurements have been repeated independently (three times) in order to verify the reproducibility of the results (repeatability). From Fig. 5, it can be seen that first, and foremost, the different LUTs can be clearly differentiated (resolved) and, secondly, there is not an appreciable change in the resonance frequency (mainly related to the dielectric constant of the LUT). The different LUTs mainly modify the magnitude of the transmission coefficient in the vicinity of resonance. This change in the magnitude of the transmission coefficient is attributed to the change of the dielectric loss (loss tangent) of the LUT. However, the dielectric constant of the different samples scarcely varies, the reason being that the PBS and the solutions of BSA in PBS are essentially water solutions, dominated by the properties of DI water. The invariability of the dielectric constant of the different liquid samples (ϵ_{LUT}) is fully justified by the fact that the resonance frequency, very sensitive to ϵ_{LUT} , does not appreciably vary in Fig. 5. Let us mention that other sensors based on active configurations have been proposed to differentiate the change in the resonance amplitude affected by the loss of the material under study [66],[67].

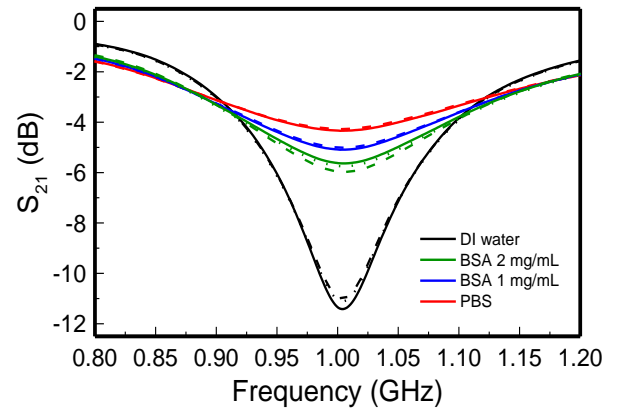


Fig. 5. Measured magnitude of the transmission coefficient for the different considered LUTs. Line with different styles (solid, dash and dot) represents independent measurements.

IV. DENATURATION OF BSA: PROTOCOL AND RESULTS

The second and main experimental validation campaign of this work has been focused on the characterization of the denaturation of BSA using the four-port structure (differential) sensor. Figure 6 shows the photograph of the sensor with the

fabricated 3D channels, including the capillaries for liquid injection. The challenge is the characterization of the denaturation process, rather than retrieving the dielectric constant and loss tangent of the LUT. Note, however, that the denaturation process of BSA in this work is activated by means of urea (acting as chaotropic agent). Thus, the presence of urea will significantly obscure the changes in the dielectric properties of BSA related to the denaturation. Consequently, since the proposed sensor is essentially a device able to detect changes in the dielectric properties of the LUT, a protocol to subtract the effects caused by the presence of urea is needed, to be discussed next. Nevertheless, let us mention that, among the several chaotropic agents, urea has been chosen to carry out the denaturation of BSA because this chaotropic substance achieves maximal solubility in the medium (when not used in large amounts), resulting in denaturation. The presence of urea causes proteins to unfold by competing and disrupting hydrogen bonds in the proteins. Preparation of an 8M urea solution has been done by introducing 4.8 g of solid urea into a 10 mL flask and filling it up with phosphate buffer (PBS). From this urea solution, concentrations of 1.5M, 3M, 4.5M and 6M were obtained by diluting the solution with different PBS volumes.

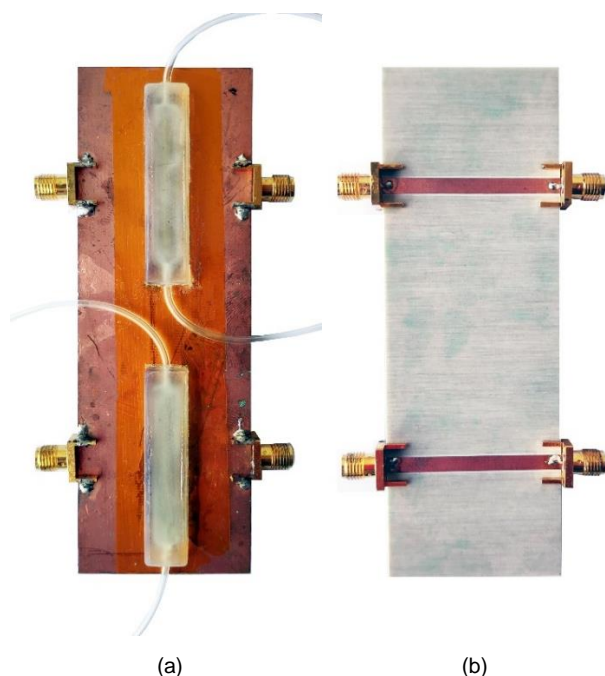


Fig. 6. Photograph of bottom (a) and top (b) views of the fabricated sensor with the 3D channels mounted on top of each sensing region.

For our experiments, two BSA solutions of 1 mg/mL and 2 mg/mL were prepared. To allow several independent tests utilizing the same original liquids, all solutions were separated into numerous replicates and kept at -2°C to conserve them. Before the beginning of the measurements, the samples were placed at room temperature for 30 minutes, while replicates were kept frozen for measurement at later stages. The measurements started by injecting the buffer solution (PBS) in the REF channel and the BSA solution at a concentration of 1

mg/mL and 2 mg/mL in the LUT channel. These measurements served as a reference during the data treatment due to the dissolved BSA in PBS. Then, the BSA 1 mg/mL was injected in the REF channel, and the mixture of the BSA 1 mg/mL and the lower urea concentrated solution (1.5M) in the LUT channel. Next, we performed the measurement by injecting BSA 2mg/mL in the REF channel and the mixture of BSA 2 mg/mL and urea at 1.5M in the LUT. Finally, the above-mentioned measurements were repeated with an increased concentration of urea (3M, 4.5M and 6M) for the two concentration of BSA (1 and 2 mg/mL). All the measurements were repeated three times independently for repeatability purposes.

Following the previous protocol to perform the measurements, the following results were obtained. Figure 7 depicts the cross-mode transmission coefficient (magnitude) for each BSA solution (at a concentration 1 mg/mL and 2 mg/mL) mixed with the different urea concentration (1.5M, 3M, 4.5M and 6M). The reference level, as stated before, was the measurement when in the REF channel was injected PBS and in the LUT channel only the BSA solution (at 1mg/mL or 2mg/mL). As it can be seen from Fig. 7, the difference in the magnitude of the cross-mode transmission coefficient from each measurement is caused by the variation of the input variable, mainly, the differential permittivity between the liquids at both channels. When PBS is injected in the REF channel and the BSA solution (in PBS) in the LUT channel, the cross-mode transmission coefficient is roughly null because there is not an appreciable difference in the dielectric properties between both liquids, thereby preserving the symmetry of the sensor structure. That is, the presence of BSA in the PBS does not alter the dielectric properties of the composite (note that such similarity between the dielectric properties of PBS and the BSA solution in PBS is naturally inferred by using differential-mode measurements). However, the symmetry is clearly truncated when urea is added in the BSA solution injected in the LUT channel. The higher the urea concentration is, the higher the cross-mode transmission coefficient (magnitude) becomes. However, measuring the cross-mode transmission coefficient from each individual BSA configuration is not enough in order to characterize the denaturation process, since the effect we are measuring is the change in the dielectric properties of the liquid, rather than the denaturation process itself. Certainly, denaturation is expected to alter the dielectric properties of the BSA solutions, but such variations are also caused by the presence of urea (note that microwave methods exhibit a limited selectivity, unless spectroscopic methods are used).

Indeed, urea, rather than the denaturation of the BSA protein, is the main cause of permittivity changes in the BSA solution. Thus, the method used to characterize the denaturation process of BSA utilizes both results (BSA 1 mg/mL and 2 mg/mL) together, rather than individually. This is necessary due to the significant effects of urea in the modification of the dielectric properties of the composites. In other words, the denaturation process cannot be detected/characterized by considering only one set of results. Nevertheless, the values of the considered

BSA concentrations (1 mg/mL and 2 mg/mL) are arbitrary. The hypothesis is that the BSA by itself is not able to generate appreciable changes in the dielectric properties of the solution with urea. Therefore, if there are changes between the results for the two sets of measurements (each one with different concentration of BSA), such differences should be attributed to the changes in the dielectric properties caused by the denaturation process. Indeed, the bounded water molecules are not expected to be equal for both sets of results. The representation of the maximum value of the magnitude of the cross-mode transmission coefficient (at 0.98 GHz) and subtracting the effect of the reference level are shown in Fig. 8. From this figure, it follows that the slope for both sets of data points is clearly different, and this should be attributed necessarily to the denaturation process. The contrast between both curves corresponds to the hydration contrast and it arises as the urea concentration increases. This conclusion is consistent with the notion that when the chaotropic substance (urea in our case) becomes more concentrated, the amount of bound water molecules increases, resulting in a higher fraction of denatured BSA. Figure 9 depicts the hydration contrast (as the difference of the cross-mode transmission coefficient) as a function of the urea concentration.

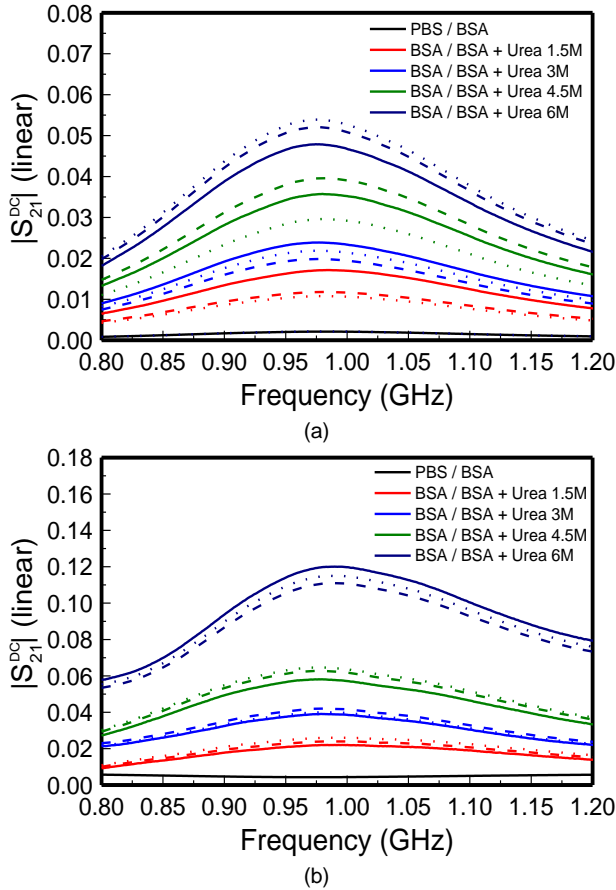


Fig. 7. Cross-mode transmission coefficient (magnitude) for each BSA solutions when mixed with different urea concentrations: (a) BSA 1 mg/mL, (b) BSA 2 mg/mL. Legend format is REF / LUT. Line with different styles (solid, dash and dot) represents independent measurements.

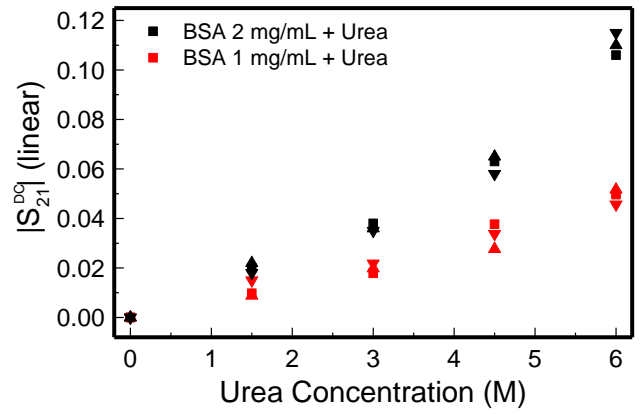


Fig. 8. Measured maximum value of the magnitude of the cross-mode transmission coefficient for both BSA solutions (1 mg/mL and 2 mg/mL) as a function of the urea concentration.

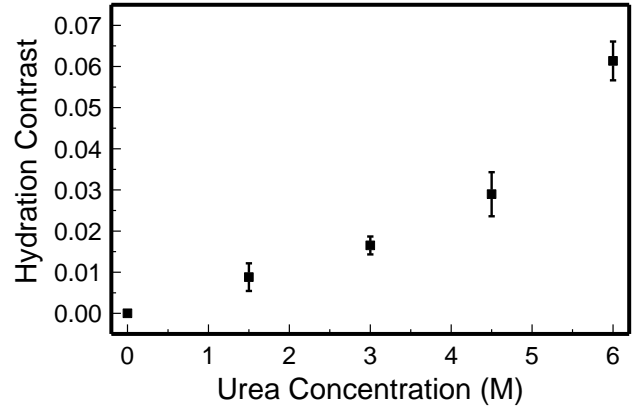


Fig. 9. Magnitude of the cross-mode transmission coefficient contrast (hydration contrast) as function of the urea concentration. Error bar represents the standard deviation of the data set, and reveal that precision is reasonably good.

V. CONCLUSIONS

In conclusion, a slot-based sensor devoted to the characterization of the denaturation process of the BSA molecule activated by urea has been reported in this paper. The sensor is a 4-port network operating in differential-mode, with two independent sensing structures, and the working principle is mode conversion caused by symmetry disruption. A protocol to detect and characterize the denaturation process has been proposed. It has been demonstrated that with the fabricated sensor, the denaturation process can be characterized, by measuring the cross-mode transmission coefficient contrast between two solutions of BSA, of different concentration. This contrast is related to the hydration of the protein in the change from the folded macromolecule to the unfolded one, due to the denaturation process. With this work it has been demonstrated that low-cost microwave sensors are useful for the characterization/detection of denaturation in proteins.

REFERENCES

- [1] S. Trabelsi et al., "New calibration technique for microwave moisture sensors," *IEEE Trans. Instrum. Meas.*, vol. 50, no. 4, pp. 877-881, 2001.

- [2] S. Trabelsi et al., "Influence of nonequilibrated water on microwave dielectric properties of wheat and related errors in moisture sensing," *IEEE Trans. Instrum. Meas.*, vol. 56, no. 1, pp. 194-198, 2007.
- [3] J. A. Satti, A. Habib, H. Anam, S. Zeb, Y. Amin, J. Loo, and H. Tenhunen, "Miniaturized humidity and temperature sensing RFID enabled tags," *Int J. RF Microw. Comput. Aided Eng.*, vol. 28, no. 1, pp. e21151, Jan. 2018.
- [4] P. Vélez, F. Martín, R. Fernández-García, and I. Gil, "Embroidered Textile Frequency-Splitting Sensor based on Stepped-Impedance Resonators," *IEEE Sensors J.*, accepted.
- [5] D. Girbau, Á. Ramos, A. Lazaro, S. Rima, and R. Villarino, "Passive wireless temperature sensor based on time-coded UWB chipless RFID tags," *IEEE Trans. Microw. Theory Techn.*, vol. 60, no. 11, pp. 3623-3632, Nov. 2012.
- [6] N. Javed, M. A. Azam, and Y. Amin, "Chipless RFID multisensor for temperature sensing and crack monitoring in an IoT environment," *IEEE Sensors Lett.*, vol. 5, no. 6, paper 6001404, Jun. 2021.
- [7] J. Naqui, M. Durán-Sindreu, and F. Martín, "Alignment and position sensors based on split ring resonators," *Sensors*, vol. 12, pp. 11790-11797, 2012.
- [8] A. Karami-Horestani, C. Fumeaux, S. F. Al-Sarawi, and D. Abbott, "Displacement sensor based on diamond-shaped tapered split ring resonator," *IEEE Sensors J.*, vol. 13, no. 4, pp. 1153-1160, Apr. 2013.
- [9] A. K. Horestani, J. Naqui, D. Abbott, C. Fumeaux, and F. Martín, "Two-dimensional displacement and alignment sensor based on reflection coefficients of open microstrip lines loaded with split ring resonators," *Electron Lett.*, vol. 50, no. 8, pp. 620-622, Apr. 2014.
- [10] A. K. Horestani, D. Abbott, and C. Fumeaux, "Rotation sensor based on horn-shaped split ring resonator," *IEEE Sens. J.*, vol. 13, pp. 3014-3015, 2013.
- [11] J. Naqui and F. Martín, "Transmission lines loaded with bisymmetric resonators and their application to angular displacement and velocity sensors," *IEEE Trans. Microw. Theory Techn.*, vol. 61, no. 12, pp. 4700-4713, Dec. 2013.
- [12] J. Mata-Contreras, C. Herrojo, and F. Martín, "Application of split ring resonator (SRR) loaded transmission lines to the design of angular displacement and velocity sensors for space applications," *IEEE Trans. Microw. Theory Techn.*, vol. 65, no. 11, pp. 4450-4460, Nov. 2017.
- [13] J. Mata-Contreras, C. Herrojo, and F. Martín, "Detecting the rotation direction in contactless angular velocity sensors implemented with rotors loaded with multiple chains of split ring resonators (SRRs)," *IEEE Sensors J.*, vol. 18, no. 17, pp. 7055-7065, Sep. 2018.
- [14] C. Herrojo, F. Muela, J. Mata-Contreras, F. Paredes, and F. Martín, "High-density microwave encoders for motion control and near-field chipless-RFID," *IEEE Sensors J.*, vol. 19, pp. 3673-3682, May 2019.
- [15] C. Herrojo, F. Paredes, and F. Martín, "Double-stub loaded microstrip line reader for very high data density microwave encoders," *IEEE Trans. Microw. Theory Techn.*, vol. 67, no. 9, pp. 3527-3536, Sep. 2019.
- [16] J. Muñoz-Enano, P. Vélez, L. Su, M. Gil, and F. Martín, "A reflective-mode phase-variation displacement sensor," *IEEE Access*, vol. 8, pp. 189565-189575, Oct. 2020.
- [17] F. Paredes, C. Herrojo, A. Moya, M. Berenguel-Alonso, D. Gonzalez, J. Bruguera, C. Delgado-Simao, and F. Martín, "Electromagnetic encoders screen-printed on rubber elevator belts and application to the measurement of cabin position and velocity," *Sensors*, vol. 22, paper 2044, 2022.
- [18] J. Muñoz-Enano, P. Vélez, M. Gil, J. Mata-Contreras, and F. Martín, "Differential-mode to common-mode conversion detector based on rat-race couplers: analysis and application to microwave sensors and comparators," *IEEE Transactions on Microwave Theory and Techniques*, vol. 68, pp. 1312-1325, April 2020.
- [19] P. Casacuberta, J. Muñoz-Enano, P. Vélez, L. Su, M. Gil, and F. Martín, "Highly sensitive reflective-mode detectors and dielectric constant sensors based on open-ended stepped-impedance transmission lines," *Sensors*, vol. 20, paper 6236, 2020.
- [20] A. Ebrahimi, W. Withayachumnankul, S. Al-Sarawi and D. Abbott, "High-Sensitivity Metamaterial-Inspired Sensor for Microfluidic Dielectric Characterization," *IEEE Sensors J.*, vol. 14, no. 5, pp. 1345-1351, May 2014.
- [21] P. Vélez, L. Su, K. Grenier, J. Mata-Contreras, D. Dubuc, and F. Martín, "Microwave microfluidic sensor based on a microstrip splitter/combiner configuration and split ring resonators (SRR) for dielectric characterization of liquids," *IEEE Sensors J.*, vol. 17, pp. 6589-6598, Oct. 2017.
- [22] J. Muñoz-Enano, P. Vélez, M. Gil, and F. Martín, "Microfluidic reflective-mode differential sensor based on open split ring resonators (OSRRs)," *Int. J. Microw. Wireless Technol.*, vol. 12, pp. 588-597, Sep. 2020.
- [23] A. Ebrahimi, F. J. Tovar-López, J. Scott, and K. Ghorbani, "Differential microwave sensor for characterization of glycerol-water solutions," *Sensors Actuators B Chem.*, vol. 321, paper 128561, Oct. 2020.
- [24] H. Y. Gan, W. S. Zhao, Q. Liu, D. W. Wang, L. Dong, G. Wang, and W. Y. Yin, "Differential microwave microfluidic sensor based on microstrip complementary split-ring resonator (MCSRR) structure," *IEEE Sensors J.*, vol. 20, no. 11, pp. 5876-5884, Jun. 2020.
- [25] L. Su, J. Mata-Contreras, P. Vélez, A. Fernández-Prieto, and F. Martín, "Analytical method to estimate the complex permittivity of oil samples," *Sensors*, vol. 18, p. 984, 2018.
- [26] P. Vélez, K. Grenier, J. Mata-Contreras, D. Dubuc, and F. Martín, "Highly-sensitive microwave sensors based on open complementary split ring resonators (OCSRRs) for dielectric characterization and solute concentration measurements in liquids," *IEEE Access*, vol. 6, pp. 48324-48338, Dec. 2018.
- [27] P. Vélez, J. Muñoz-Enano, K. Grenier, J. Mata-Contreras, D. Dubuc, F. Martín, "Split ring resonator (SRR) based microwave fluidic sensor for electrolyte concentration measurements," *IEEE Sensors J.*, vol. 19, no. 7, pp. 2562-2569, Apr. 2019.
- [28] E. Levy, G. Barshtein, L. Livshitz, P. Ben Ishai and Y. Feldman, "The Vitality of Human RBC and its connection to cytoplasmic water: I. The glucose concentration influence," *J. Physical Chemistry B*, vol. 120, pp. 10214, 2016.
- [29] F. Artis, T. Chen, T. Chrétiennot, J.-J. Fournié, M. Poupot, D. Dubuc, K. Grenier, "Microwaving biological cells - Intracellular analysis with microwave dielectric spectroscopy," *IEEE Microw. Mag.*, vol. 16, no. 4, pp. 87-96, May 2015.
- [30] K. Grenier, G. Pratiel, H. Mazur and D. Dubuc, "Detection of a Macromolecule Denaturation With Microwave Dielectric Spectroscopy based on Hydration Modifications," *2020 IEEE MTT-S International Microwave Biomedical Conference (IMBioC)*, 2020, pp. 1-4, Dec 14-17 Toulouse, France.
- [31] Y. Feldman et al., "Hydration of AMP and ATP Molecules in Aqueous Solution and Solid Films," *Int. J. Mol. Sci.*, vol. 14, pp. 22876-22890, 2013.
- [32] K. Fuchs, U. Kaatze, "Molecular Dynamics of Carbohydrate Aqueous Solutions. Dielectric Relaxation as a Function of Glucose and Fructose Concentration," *J. Phys. Chem. B*, vol. 105, pp. 2036-2042, 2001.
- [33] K. Fuchs, U. Kaatze, "Dielectric spectro of mono- and disaccharide aqueous solutions," *J. Chem. Phys.*, vol. 116, no. 16, 7137-7144, 2002.
- [34] C. Cametti, S. Marchetti, C.M.C. Gambi, G. Onori, "Dielectric relaxation spectroscopy of lysozyme aqueous solutions: analysis of the δ -dispersion and the contribution of the hydration water," *J. Phys. Chem. B*, vol. 115, pp. 7144-7153, 2011.
- [35] Y. Hayashi, I. Oshige, Y. Katsumoto, S. Omori, A. Yasuda, "Protein-solvent interaction in urea-water systems studied by dielectric spectroscopy," *J. Non-Crystalline Solids*, vol. 353, pp. 4492-4496, 2007.
- [36] B.A. Mazzeo, A.J. Flewitt, "Observation of protein-protein interaction by dielectric relaxation spectroscopy of protein solutions for biosensor application," *Appl. Phys. Lett.*, vol. 90, paper 123901, 2007.
- [37] K. Grenier, G. Pratiel, H. Mazur and D. Dubuc, "Detection of a Macromolecule Denaturation With Microwave Dielectric Spectroscopy based on Hydration Modifications," *2020 IEEE MTT-S International Microwave Biomedical Conference (IMBioC)*, 2020, pp. 1-4.
- [38] G. Galindo-Romera, F. Javier Herraiz-Martínez, M. Gil, J. J. Martínez-Martínez and D. Segovia-Vargas, "Submersible Printed Split-Ring Resonator-Based Sensor for Thin-Film Detection and Permittivity Characterization," *IEEE Sensors J.*, vol. 16, no. 10, pp. 3587-3596, May 2016.
- [39] A. Nuñez-Flores, P. Castillo-Aranibar, A. García-Lampérez, and D. Segovia-Vargas, "Design and Implementation of a Submersible Split Ring Resonator Based Sensor for Pisco Concentration Measurements," *2018 IEEE MTT-S Latin America Microwave Conference (LAMC 2018)*, Arequipa, Peru, Dec. 2018.
- [40] E. Reyes-Vera, G. Acevedo-Osorio, M. Arias-Correa, and D. E. Senior, "A submersible printed sensor based on a monopole-coupled split ring resonator for permittivity characterization," *Sensors*, vol. 19, Apr. 2019.
- [41] R. Kumaran and P. Ramamurthy, "Denaturation Mechanism of BSA by Urea Derivatives: Evidence for Hydrogen-Bonding Mode from Fluorescence Tools," *Journal of Fluorescence*, vol. 21, no. 4, pp. 1499-1508, Jul. 2011.
- [42] D. M. Togashi, A. G. Ryder, and D. O'Shaughnessy, "Monitoring local unfolding of bovine serum albumin during denaturation using steady-state and time-resolved fluorescence spectroscopy," *Journal of Fluorescence*, vol. 20, no. 2, pp. 441-52, Mar 2010.

- [43] J. Muñoz-Enano, P. Vélez, M. Gil, E. Jose-Cunilleras, A. Bassols, and F. Martín, "Characterization of Electrolyte Content in Urea Samples through a Differential Microfluidic Sensor Based on Dumbbell-Shaped Defect Ground Structures", *Int. J. Microw. Wireless Technol.*, vol. 12(9), pp. 817-824, 2020.
- [44] A. Ebrahimi, J. Scott and K. Ghorbani, "Differential Sensors Using Microstrip Lines Loaded With Two Split-Ring Resonators," *IEEE Sensors J.*, vol. 18, no. 14, pp. 5786-5793, Jul. 2018.
- [45] A. Ebrahimi, J. Scott and K. Ghorbani, "Transmission Lines Terminated With LC Resonators for Differential Permittivity Sensing," *IEEE Microw. Wireless Compon. Lett.*, vol. 28, no. 12, pp. 1149-1151, Dec. 2018.
- [46] A. Ebrahimi, G. Beziuk, J. Scott, and K. Ghorbani, "Microwave Differential Frequency Splitting Sensor Using Magnetic-LC Resonators," *Sensors*, vol. 20, no. 4, paper 1066, 2020.
- [47] J. Muñoz-Enano, P. Vélez, M. Gil, and F. Martín, "Planar microwave resonant sensors: a review and recent developments," *Appl. Sciences*, vol. 10, p. 2615 (29 pages), 2020.
- [48] M. S. Boybay and O. M. Ramahi, "Material characterization using complementary split-ring resonators," *IEEE Trans. Instrum. Meas.*, vol. 61, no. 11, pp. 3039-3046, Nov. 2012.
- [49] C. S. Lee and C. L. Yang, "Complementary split-ring resonators for measuring dielectric constants and loss tangents," *IEEE Microw. Wireless Compon. Lett.*, vol. 24, no. 8, pp. 563-565, Aug. 2014.
- [50] W. Withayachumnankul, K. Jaruwongrungssee, A. Tuantranont, C. Fumeaux, and D. Abbott, "Metamaterial-based microfluidic sensor for dielectric characterization", *Sens. Actuators A*, vol. 189, pp. 233-237, 2013.
- [51] A. Salim and S. Lim, "Complementary split-ring resonator-loaded microfluidic ethanol chemical sensor", *Sensors*, vol 16, paper 1802, 2016.
- [52] C. L. Yang, C. S. Lee, K. W. Chen, and K. Z. Chen, "Noncontact measurement of complex permittivity and thickness by using planar resonators," *IEEE Trans. Microw. Theory Techn.*, vol. 64, no. 1, pp. 247-257, Jan. 2016.
- [53] M. Abdolrazzaghi, M. H. Zarifi, and M. Daneshmand, "Sensitivity enhancement of split ring resonator based liquid sensors," *2016 IEEE Sensors*, Orlando, FL, USA, 30 Oct.-3 Nov. 2016.
- [54] M. Abdolrazzaghi, M. H. Zarifi, W. Pedrycz, and M. Daneshmand, "Robust ultra-high resolution microwave planar sensor using fuzzy neural network approach," *IEEE Sens. J.*, vol. 17, pp. 323-332, 2016.
- [55] M. H. Zarifi and M. Daneshmand, "Monitoring solid particle deposition in lossy medium using planar resonator sensor," *IEEE Sens. J.*, vol. 17, pp. 7981-7989, 2017.
- [56] M. H. Zarifi, S. Deif, M. Abdolrazzaghi, B. Chen, D. Ramsawak, M. Amyotte, N. Vahabisani, Z. Hashisho, W. Chen, and M. Daneshmand, "A microwave ring resonator sensor for early detection of breaches in pipeline coatings," *IEEE Trans. Ind. Electron.*, vol. 65, pp. 1626-1635, 2017.
- [57] M. Abdolrazzaghi, M. Daneshmand, and A. K. Iyer, "Strongly enhanced sensitivity in planar microwave sensors based on metamaterial coupling," *IEEE Trans. Microw. Theory Techn.*, vol. 66, pp. 1843-1855, 2018.
- [58] J. Muñoz-Enano, P. Vélez, L. Su, M. Gil, P. Casacuberta and F. Martín, "On the Sensitivity of Reflective-Mode Phase-Variation Sensors Based on Open-Ended Stepped-Impedance Transmission Lines: Theoretical Analysis and Experimental Validation," *IEEE Trans. Microw. Theory Techn.*, vol. 69, no. 1, pp. 308-324, Jan. 2021.
- [59] L. Su, J. Muñoz-Enano, P. Vélez, P. Casacuberta, M. Gil, and F. Martín "Highly Sensitive Phase Variation Sensors Based on Step-Impedance Coplanar Waveguide (CPW) Transmission Lines", *IEEE Sensors J.*, vol. 21, no. 3, pp. 2864-2872, Feb. 2021.
- [60] L. Su, J. Muñoz-Enano, P. Vélez, M. Gil, P. Casacuberta, and F. Martín, "Highly sensitive reflective-mode phase-variation permittivity sensor based on a coplanar waveguide (CPW) terminated with an open complementary split ring resonator (OCSRR)", *IEEE Access*, vol. 9, pp. 27928-27944, 2021.
- [61] J. Muñoz-Enano, J. Coromina, P. Vélez, L. Su, M. Gil, P. Casacuberta, and F. Martín, "Planar phase-variation microwave sensors for material characterization: a review and comparison of various approaches", *Sensors*, vol. 21, paper 1542, 2021.
- [62] L. Su, J. Muñoz-Enano, P. Vélez, P. Casacuberta, M. Gil, F. Martín, "Phase-Variation Microwave Sensor for Permittivity Measurements Based on a High-Impedance Half-Wavelength Transmission Line", *IEEE Sensors J.*, vol. 21, no. 9, pp. 10647-10656, May 2021.
- [63] J. Muñoz-Enano, J. Martel, P. Vélez, F. Medina, L. Su, and F. Martín, "Parametric analysis of the edge capacitance of uniform slots and application to frequency-variation permittivity sensors", *Appl. Sci.*, vol. 11, paper 7000, 2021.

- [64] D. M. Pozar, *Microwave Engineering*, 4th Ed., John Wiley, Hoboken, NJ, USA, 2012.
- [65] F. Martín, L. Zhu, J. Hong, and F. Medina, *Balanced Microwave Filters*, Wiley/IEEE Press, Hoboken, NJ, USA, 2018.
- [66] M. Abdolrazzaghi, N. Katchinskiy, A. Y. Elezzabi, P. E. Light and M. Daneshmand, "Noninvasive Glucose Sensing in Aqueous Solutions Using an Active Split-Ring Resonator," *IEEE Sensors J.*, vol. 21, no. 17, pp. 18742-18755, Sep. 2021.
- [67] N. Kazemi, K. Schofield, and P. Musilek, "A High-Resolution Reflective Microwave Planar Sensor for Sensing of Vanadium Electrolyte," *Sensors*, vol. 21, no. 11, paper 3759, 2021.



Jonathan Muñoz-Enano (S'19) was born in Mollet del Vallès (Barcelona), Spain, in 1994. He received the Bachelor's Degree in Electronic Telecommunications Engineering in 2016 and the Master's Degree in Telecommunications Engineering in 2018, both at the Autonomous University of Barcelona (UAB). Actually, he is working in the same university in the elaboration of his PhD, which is focused on the development of microwave sensors based on metamaterials concepts for the dielectric characterization of materials and biosensors.



Olivia Peytral-Rieu (S'20) received the M.S. degree in translational medicinal chemistry from University of Montpellier, Montpellier, France, in 2019; Engineering Degree in chemistry, biology and health from the Engineering Chemistry School of Montpellier, Montpellier, France, in 2019 and B.S. in general chemistry from the Engineering Chemistry School of Montpellier, Montpellier, France, 2017. She is currently pursuing the Ph.D. degree at the University of Toulouse, Toulouse, France. She is currently with the Laboratory of Analysis and Architecture of System, National Scientific Research Center, Toulouse. Her current research interests include the use of microwave based dielectric spectroscopy for the study and the characterization of microtissues.



Paris Vélez (S'10-M'14-SM'21) was born in Barcelona, Spain, in 1982. He received the degree in Telecommunications Engineering, specializing in electronics, the Electronics Engineering degree, and the Ph.D. degree in Electrical Engineering from the Universitat Autònoma de Barcelona, Spain, in 2008, 2010, and 2014, respectively. His Ph.D. thesis concerned common mode suppression differential microwave circuits based on metamaterial concepts and semi-lumped resonators. During the Ph.D., he was awarded with a pre-doctoral teaching and research fellowship by the Spanish Government from 2011 to 2014. From 2015-2017, he was involved in the subjects related to metamaterials sensors for fluidics detection and characterization at LAAS-CNRS through a TECNIO Spring fellowship cofounded by the Marie Curie program. From 2018 to 2020 he has worked in miniaturization of passive circuits RF/microwave and sensors-based metamaterials through Juan de la Cierva fellowship. His current research interests include the miniaturization of passive circuits RF/microwave and sensors-based metamaterials. Dr. Vélez is a Reviewer for the IEEE Transactions on Microwave Theory and Techniques and for other journals.



David Dubuc (S'99-M'03) received the Agregation degree from the Ecole Normale Supérieure de Cachan, Paris, France, in 1996, and the M.S. and Ph.D. degrees in electrical engineering from the University of Toulouse, Toulouse, France, in 1997 and 2001, respectively. From 2002 to 2013, he was an Associate Professor with the University of Toulouse, and a Researcher with the Laboratory of Analysis and Architecture of System of National Scientific Research Center, Toulouse, France. From 2007 to 2009, he was a Visiting Senior Researcher with the Laboratory of Integrated Microelectronic Systems, CNRS/Institute of Industrial Science, The University of Tokyo, Tokyo, Japan. Since 2013, he is Professor at the University of Toulouse. His research interests include the development

of microwave circuits integrated due to microtechnologies and their application to wireless telecommunication and biology. He has participated or organized several international events, including GAAS 2005 and the 2020 MTT-S International Microwave Biomedical Conference (IMBioC 2020), where he acted as Topical Committee Chair.

Prof. Dubuc is a member of the IEEE Microwave Theory and Techniques Society (IEEE MTT-S), and of the European Microwave Association (EuMA). He is reviewer of several journals, including IEEE journals such as IEEE Transactions on Microwave Theory and Techniques, IEEE Microwave and Wireless Components Letters, and IEEE Sensors Journal, among others.



Katia Grenier (S'99–M'03) received the M.S. and Ph.D. degrees in electrical engineering from the University of Toulouse, Toulouse, France, in 1997 and 2000, respectively. She was engaged in microelectromechanical systems circuits on silicon. She was a Post-Doctoral Fellow with Agere Systems (Nokia Bell Labs). In 2001, she joined the Laboratory of Analysis and Architecture of System of the National Scientific Research Center CNRS (LAAS-CNRS), Toulouse, France. From 2007 to 2009, she was with the Laboratory for Integrated Micromechatronic Systems, CNRS/Institute of Industrial Science, The University of Tokyo, Tokyo, Japan, where she was engaged in launching research activities on microwave-based biosensors. Her research interests in LAAS-CNRS are currently focused on the development of fluidic-based microsystems, notably for biological and medical applications at the molecular, cellular and tissue levels. She is the head of the High Frequency and Fluidic Micro-nanosystems Group (MH2F Group) at LAAS-CNRS. She has participated or organized several international events, including Workshops at the IEEE International Microwave Symposium (2013 and 2016), a Women in Microwave event (at IMS 2018), and the 2020 IEEE MTT-S International Microwave Biomedical Conference (IMBioC 2020), where she has acted as General Chair. She has acted as Guest Editor in several Special Issues in IEEE T-MTT and IEEE J-ERM. Dr. Grenier is also a member of the IEEE MTT-28 Technical Committee on Biological Effects and Medical Applications of RF and Microwave of the IEEE Microwave Theory and Techniques Society.



Ferran Martín (M'04-SM'08-F'12) was born in Barakaldo (Vizcaya), Spain in 1965. He received the B.S. Degree in Physics from the Universitat Autònoma de Barcelona (UAB) in 1988 and the PhD degree in 1992. From 1994 up to 2006 he was Associate Professor in Electronics at the Departament d'Enginyeria Electrònica (Universitat Autònoma de Barcelona), and since 2007 he is Full Professor of Electronics. In recent years, he has been involved in different research activities

including modelling and simulation of electron devices for high frequency applications, millimeter wave and THz generation systems, and the application of electromagnetic bandgaps to microwave and millimeter wave circuits. He is now very active in the field of metamaterials and their application to the miniaturization and optimization of microwave circuits and antennas. Other topics of interest include microwave sensors and RFID systems, with special emphasis on the development of high data capacity chipless-RFID tags. He is the head of the Microwave Engineering, Metamaterials and Antennas Group (GEMMA Group) at UAB, and director of CIMITEC, a research Center on Metamaterials supported by TECNIO (Generalitat de Catalunya). He has organized several international events related to metamaterials and related topics, including Workshops at the IEEE International Microwave Symposium (years 2005 and 2007) and European Microwave Conference (2009, 2015 and 2017), and the Fifth International Congress on Advanced Electromagnetic Materials in Microwaves and Optics (Metamaterials 2011), where he acted as Chair of the Local Organizing Committee. He has acted as Guest Editor for six Special Issues on metamaterials and sensors in five International Journals. He has authored and co-authored over 650 technical conference, letter, journal papers and book chapters, he is co-author of the book on Metamaterials entitled *Metamaterials with Negative Parameters: Theory, Design and Microwave Applications* (John Wiley & Sons Inc.), author of the book *Artificial Transmission Lines for RF and Microwave Applications* (John

Wiley & Sons Inc.), co-editor of the book *Balanced Microwave Filters* (Wiley/IEEE Press) and co-author of the book *Time-Domain Signature Barcodes for Chipless-RFID and Sensing Applications* (Springer). Ferran Martín has generated 21 PhDs, has filed several patents on metamaterials and has headed several Development Contracts.

Prof. Martín is a member of the IEEE Microwave Theory and Techniques Society (IEEE MTT-S). He is reviewer of the IEEE Transactions on Microwave Theory and Techniques and IEEE Microwave and Wireless Components Letters, among many other journals, and he serves as member of the Editorial Board of IET Microwaves, Antennas and Propagation, International Journal of RF and Microwave Computer-Aided Engineering, and Sensors. He is also a member of the Technical Committees of the European Microwave Conference (EuMC) and International Congress on Advanced Electromagnetic Materials in Microwaves and Optics (Metamaterials). Among his distinctions, Ferran Martín has received the 2006 Duran Farell Prize for Technological Research, he holds the *Parc de Recerca UAB – Santander Technology Transfer Chair*, and he has been the recipient of three ICREA ACADEMIA Awards (calls 2008, 2013 and 2018). He is Fellow of the IEEE and Fellow of the IET.